Hydrological behaviour of earthflows developed in clay-shales: Investigation, concept and modelling

Jean-Philippe Malet, Olivier Maquaire, Theo van Asch

HYDROLOGICAL BEHAVIOUR OF EARTHFLOWS DEVELOPPED IN CLAY-SHALES. INVESTIGATION, CONCEPT AND MODELLING.

J.-P. MALET, O. MAQUAIRE
Institut de Physique du Globe, UMR 7516 CNRS-ULP, 5, rue René Descartes, F-67084 Strasbourg Cedex, France

Th.W.J. VAN ASCH
Centre of the Environment and Landscape Dynamics, Heidelberglaan 2, P.O. Box 80115, 3508 TC Utrecht, The Netherlands

ABSTRACT: This paper focuses on the hydro(geo)logical temporal behaviour of deep-seated earthflows developed in clay-shales of Southeast France. These landslides experience a remarkable seasonal kinematical trend, controlled by ground water recharge and rainfall. The first part of the manuscript discusses the data necessary to acquire to build a concept for the hydrological behaviour of earthflows. The second part focuses on the implementation of this concept in a hydrological model, and discusses its calibration and validation. A coupled unsaturated/saturated model, incorporating Darcian saturated flow, fissure flow and meltwater flow has been developed to represent the landslide hydrology. The conceptual model is formalized in a 2.5-D physically-based and spatially distributed scheme. The model is calibrated and validated on the multi-parameters database acquired on the site since 1996. The complex time-dependent and three-dimensional groundwater regime is well described, on both short- and long-term. Once calibrated, the model can be used to simulate the landslide hydrological behaviour in real or hypothetical situations and help to predict future scenarios based on environmental change.

Keywords: earthflow, hydrology, physically-based modelling, investigation, clay-shales

1 FOREWORD

- What changes can be expected in the activity of large flow-like landslides in the future under the impact of environmental changes?
- How will a change in landslide topography affect the water table along all the landslide body?
- What are the most active processes governing the recharge of a landslide groundwater table and the thresholds triggering an acceleration of the displacements?

Slope stability engineers are often called upon to predict the behaviour of landslide complexes by answering questions like these. Majority of the landslide triggering mechanisms is related to hydro(geo)logical triggering, induced by rainfall or snowmelt. Hydrological triggering can be defined (1) as the reduction of the safety factor of a slope to unity as a result of decrease in shear strength due to an increase in pore-water pressure, or (2) as the progressive building of fully saturated conditions in a slope inducing the overlap of the yield stress and the initiation of flow-like phenomena. Providing answers to the above mentioned simple questions involves formulating a correct conceptual model, selecting parameter values to describe spatial variability within the groundwater flow system, as well as spatial and temporal trends in hydrologic stresses and past and future trends in water levels (Merrien-Soukatchoff, 2002; Ambroise, 1999; Anderson and Woessner, 1992). Although some decisions can be made using best engineering or best geologic judgment, in many instances human reasoning alone is inadequate to synthesize the conglomeration of factors involved in analyzing complex groundwater problems. The best tool to help slope stability engineers meet the challenge of prediction is usually a landslide hydrological model, describing the relations between climate characteristics (inputs) and groundwater response (outputs).

Surprisingly, modelling the hydrological factors which control landslides has been curiously slow to gain acceptance (Anderson and Kemp, 1988), compared to rainfall-runoff modelling or watershed hydrological modelling. Nevertheless, this aspect has been gaining ground in recent years as geotechnical, geomorphological and hydrological models are drawn closer together. The research frontiers are connected with the complexity of real landslides, the difficulty to survey the piezometric levels, or the soil moisture in 'moving environments', the difficulty to understand the water pathways within the landslide bodies, or the inability of the models to handle large complex systems with 3-D effects (Brunsden, 1999). A variety of theoretical studies have clarified the destabilizing role of steady Darcian groundwater flow in slopes (Hodge and Freeze, 1977; Iverson and Major, 1986). Only recently, however, have quantitative studies addressed the destabilizing role of transiently recharging ground water flow (Iverson *et al.*, 1997; Ng and Shi, 1998; Brooks *et al.*, 2002), and these studies typically have focussed on short-term water-table fluctuations. Few, if any, studies have focussed on spatially variable transient ground water flow that repeatedly affects the hydrological behaviour of landslides or have focussed on the validation of saturated/unsaturated models on long high temporal resolution time series (Ridolf *et al.*, 2003).

The recent development of multi-parameters distributed databases (rainfall, temperature, capillary pressure head, soil moisture, ground water level) on several landslides (*La Clapière, Séchilienne* in France; *Tessina, Corvara, Alvéra, Rossone* in Italy; *Vallcebre* in Spain, etc), especially in Europe, allows the calibration and the validation of physically-based models (essentially 1-D or 2-D, more rarely 3-D). The scientific community has developed many models (Corominas, 1998) and the object of this article is to demonstrate the potential of dynamic distributed models. Therefore, the primary objective of this study is to investigate the possibility of including more temporal and spatial information on short- and long-term landslide hydrology forecast, which is not easily attained in the traditional time-series model or conceptual hydrological models. This work resulted in the drafting of specifications for modelling these phenomena. Because of their complexity a 'realistic' numerical simulation calls for the addition of a hydrological model (rainfall-groundwater relationship) to a geomechanical model (groundwater-deformation relationship) by a material behaviour law. Because of the wide variability in the quantity of water stored in the saturated and unsaturated zones and the comparatively few return periods of critical rainy episodes the behaviour of landslides

seems to be mainly governed by the hydrological system (Freeze, 1987; Anderson et al, 1988). Many authors (Haneberg, 1991; Van Asch *et al.*, 1999) have shown that the quality of the hydrological model had a greater influence on the general behaviour model than geomechanical modelling. Other authors have also insisted on the need to describe the behaviour of saturated and non-saturated flows or to introduce the effects of macropores and fissures (Keefer and Johnson, 1983; Van Asch *et al.*, 1999).

In this paper we present results of a detailed hydrological and geomorphological investigation of the Super-Sauze earthflow, one of the persistently active landslide occurring in clay-rich material of the French Alps (Malet *et al.*, 2003a). The earthflow moves significant distances each rainy season: however, the timing, duration, and speed of movement do not correlate directly with the timing and amount of rainfall (Malet *et al.*, 2002). The unsaturated zone strongly attenuates and delays the precipitation. The seasonality of ground water recharge implies that only in the case of a moist unsaturated zone, recharge occurs during rain events, and consequently that snowmelt water has a considerable influence on the recharge. Therefore a coupled unsaturated/saturated model is needed for landslides in such material. Also, the recharge through a fine clay-silt surface material with low matric permeability is facilitated by preferential fissure flow paths. A concept for the temporal behaviour of these earthflows is proposed, and implemented in a distributed physically-based hydrological model, managing the complex 3-D geometry and incorporating fissure flow and snowmelt. The model is calibrated and extensively validated at the field scale. Two practical uses of the model for hazard assessment and risk mitigation are then presented.

2 MODELLING STRATEGY AND POTENTIAL OF DISTRIBUTED PHYSICALLY-BASED MODELS

There are almost as many different models as there are listed types of landslide, so it is useful to clarify certain terms, in order to get a clear picture of landslide models, which are often redundant. A landslide hydrological model is any type of device that represents an approximation of a landslide hydrological situation. A mathematical hydrological model simulates groundwater flow indirectly by means of a governing equation thought to represent the physical processes that occur in the landslide system, together with equation that describes heads or flows along the boundaries of the model (boundary conditions). For time-dependent problems, an equation describing the initial distribution of heads and soil moisture contents in the landslide is also needed (initial conditions). Mathematical models can be solved analytically or numerically. When assumptions used to derive an analytical solution are judged to be too simplistic and inappropriate for the problem under consideration, a numerical model may be selected. Generally speaking, the fewer the simplifying assumptions used to formulate a model, the more complex is the model. Finally, the sets of commands used to solve a mathematical model on a computer forms the computer program or code. The code is generic, whereas a model includes a set of boundary and initial conditions as well as a site-specific grid and site-specific parameter values (Anderson and Woessner, 1992; Merrien-Soukatchoff, 2002).

It is essential to identify clearly the purpose of the modelling effort at the onset of the study, and to establish a modelling strategy. A strategy for modelling includes concept definition, code selection and formulation, model design, calibration, sensitivity analysis and finally prediction (Fig. 1). Each of these steps builds support in demonstrating that a given site-specific model is capable of producing meaningful results, i.e. that the model is valid.

In particular, the definition of a conceptual model of the landslide system, and code selection are of paramount importance (Van Asch *et al.*, 1999). The response time of a landslide to precipitation is dependent on the hydrological processes which influence the transmission of the precipitation input to the depth of the unstable mass. As a consequence different types of landslides have different hydrological systems and react at different temporal scales to the net precipitation input. Therefore, the first step of the development and implementation of hydrological models to landslide is the analyses of the "rain-groundwater" relation, on the basis of long duration time series and fieldwork. Much data processing is therefore necessary to build a concept for the temporal behaviour of the landslide (Collinson and Anderson., 1998). This includes: the reconstruction of landslide geometry (topography, landslide bottom, internal structure), the definition of aquifer (permeability, retention capacity, porosity, transmissitivity) and soil properties, the influence of the spatial variability of the soil and aquifer properties, the identification of mass balance factors (inputs and outputs) and the influence of the different factors on water table fluctuations. Hydrological units and landslide system boundaries must be identified.

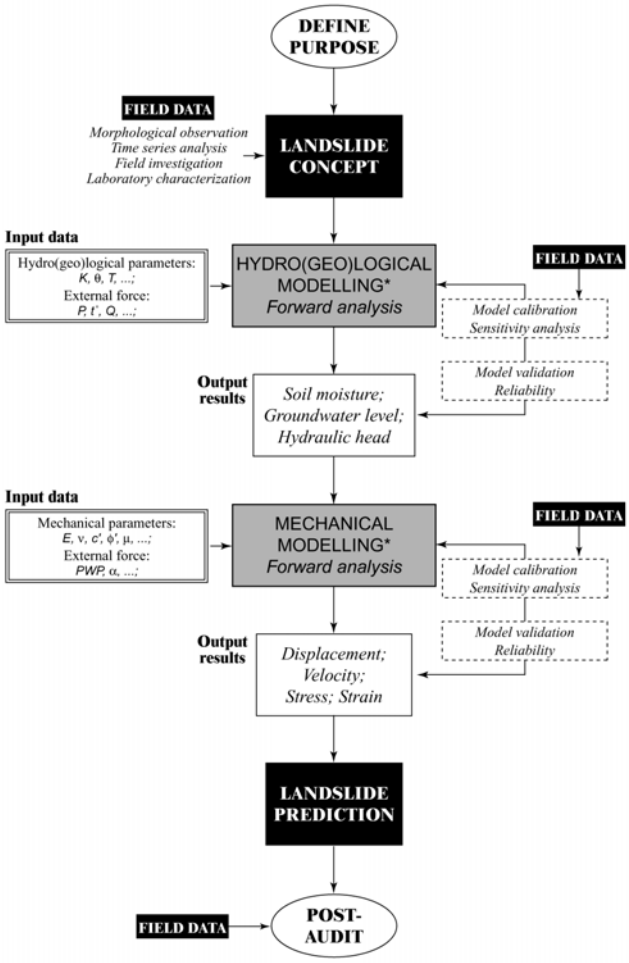

Figure 1. Steps in a protocol for landslides model applications (modified after Anderson and Woessner, 1992).

Code selection implies the choice of the best algorithms and the most adapted geometrical schematisation to solve the mathematical model numerically. If most of the research has focussed on the temporal behaviour of shallow landslides whose hydrological system is controlled by the travel time of the precipitation input through the unsaturated zone of the topsoil (Van Beek and Van Asch, 1999), or on the mechanics of deep-seated landslides controlled by saturated conditions, fewer research have focused on the landslides governed by both saturated and unsaturated conditions. This coupling is particularly needed for the analysis of landslides occurring in fine-grained (silt-clay) material, such as marls, clays or clay-shales. The traditional approach of modelling the piezometer responses involves an overall representation in which mean rainfall inputs and average hydrological parameters (permeability, porosity etc.) are used as

input variables. The types of code applicable are more or less complex, depending on the objectives, from simple 1-D lumped models to complex physically-based 2-D or 3-D calculation codes for saturated and unsaturated flows. This gives us an understanding of the value of distributed approaches, either 2-D or 3-D, which enable us to take account of the spatial variability of the landslide material, of the topographic control on the convergence of flows, or to divide the hydrological system into hydrological units (Miller and Sias 1998). They enable us to simulate the land cover evolution and the extent to which an unstable site is fissured (Van Beek, 2002). Finally their spatial character enables us to study the influence of the location of mitigation works (drainage trenches etc.) and ecological engineering (type, distribution, density of plantations) on the landslide hydrological regime. This research attempts to test, calibrate and validate such codes for complex landslides affecting fine-grained material, characterized by saturated and unsaturated conditions.

3 FIELD SETTING AND DATA COLLECTION

3.1 *Morphological and geological context*

Deep-seated earthflows are the most typical landslides involving weathered black marl (Callovo-Oxfordian) in the Southeastern part of the French Alps (Malet and Maquaire, 2003). They are generally the result of catastrophic failures in which the initial structural rock block slides transform into a fast moving massive translational landslide progressing downslope, often in natural stream channels. Their movements may result from sliding and flowing, either singly or in combination. Such multiple-mode slope movements exhibit a rapid or slower intermittent movement influenced by slope morphology, rock mass fabric, and hydrology (Hungr *et al.*, 2001).

In the Barcelonette Basin, about 100 km north of Nice, three large earthflows (Poche, Super-Sauze and La Valette) have occurred. These earthflows are very active and localized in torrential basins (Fig. 2a). All three landslides are typical earthflows in an intermediate stage of evolution (between stage B and C, -Giusti *et al.*, 1996-) with morphological features clearly recognisable. The length of the earthflows reaches 1100 m at *Poche*, 800 m at *Super-Sauze*, and 1800 m at *La Valette*. The accumulation zone presents an average slope of 20° for *Poche*, 25° for *Super-Sauze*, and 28° for *La Valette*. Finally, a terminal lobe dominates the lowermost part of the earthflows. *Poche* and *Super-Sauze* earthflows are bordered by lateral streams, draining the groundwater tables and adding the contribution of some erosion to the others factors governing the landslide movement. The total volume is estimated at 700,000 to 900,000 m^3 for Poche, 750,000 m^3 for Super-Sauze and over 3,500,000 m^3 for *La Valette*. Over the period 1992-2002, the displacements reached 130 m for Poche, 145 m for *La Valette*, and 160 m for *Super-Sauze*. It is worth noting that the maximal annual displacements are reached for the wettest years of this period, showing the hydro-climatic control of these landslides

Among these earthflows, the *Super-Sauze* earthflow is surveyed by the *Institut de Physique du Globe, Ecole et Observatoire des Sciences de la Terre (Strasbourg, France)* since 1991. It affects the north-facing slope of the Brec Second crest in the 'Roubine' area, a 75 ha area of badlands cut in black marls (Fig. 2b, 2c). The combination of steep slopes (up to 35°), downslope stratigraphic dip and absence of vegetation makes this basin one of the most landslide, flow and debris-flow prone areas in the Barcelonnette Basin. The earthflow has a characteristic morphology of blocks and panels of marls that fail the main scarp (2105 m) by plane ruptures, accumulate, progressively deform and result in a heterogeneous flow-like tongue (Fig. 2a). Uphill, the main scarp, inclined at approximately 70°, cuts into morainal deposits (about ten meters thick) and subjacent *in-situ* black marls steep slopes about 100 m high. Immediately below the main scarp, the so-called 'upper-shelf' appears as a block field, with black marls panels and dihedrons more or less buried in a very heterogeneous formation (Fig. 2d, 2e). The reworked material then transforms into a flow over a distance of almost 500 m. Progressing downstream, an area of dislocated and disintegrating blocks passes to an uneven, rough, surface of crumbling blocks and finally to a slightly uneven surface scattered with calcite and moraine pebbles, weathered stones and flakes of various sizes. The intermediate slopes on this section range up 20 to 25°. The relatively rectilinear profile is interrupted downstream by the slight convexity of the 'lower shelf'. The toe of the moving mass is presently at an altitude of 1740 m. Tension cracks and shear cracks (Fig. 2f, 2g) are characteristic features of such earthflows. Surface drainage operates in small gullies, rills and an axial main intra-flowing gully with an intermittent run-off, and in two lateral gullies with perennial run-off (Fig. 2h). Flow varies greatly with the season and the hydro-climatic conditions (Malet *et al.*, 2002). Their role is significant in drainage and particularly in erosive action. Different soil surface characteristics are clearly recognisable (Fig. 2i, 2j).

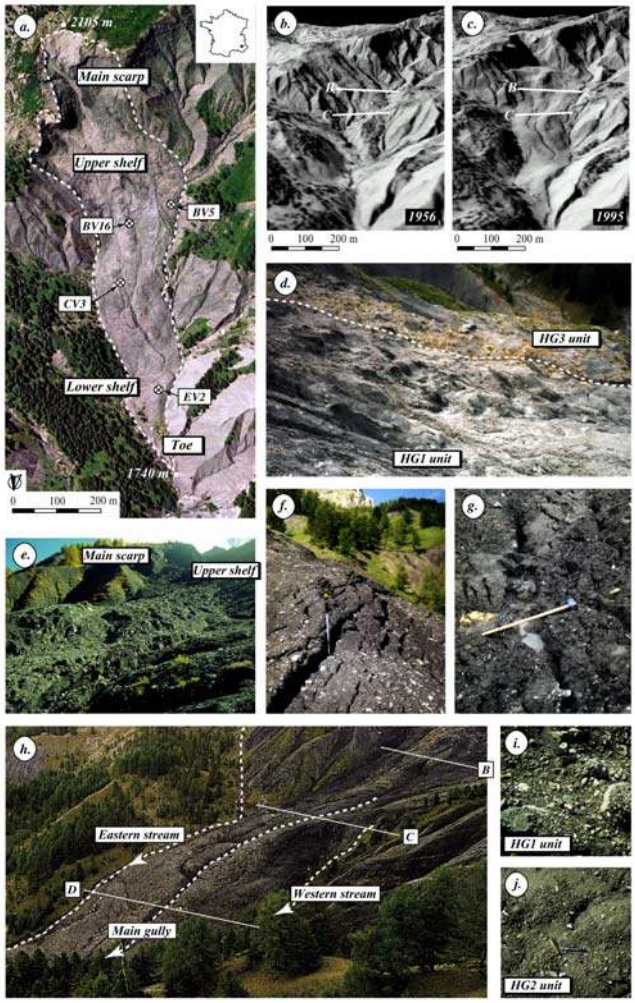

Figure 2. Morphological sketch of the Super-Sauze earthflow. (a): aerial ortho-photograpgs of the earthflow, (b), (c): original topography pre-failure topography in 1956, and earthflow development in 1995, (d), (e): hummocky topography in the ablation zone of the earthflow, (f), (g): open and saturated tension crack in the upper part of the earthflow, (h): track of the earthflow and location of the drainage channels, (i), (j): detail of the soil surface characteristics of the earthflow.

3.2 *Constraints and investigation strategies*

Observations and measurements began in 1991: characterisation of the earthflow kinematic by the periodic survey of a topometric network (Flageollet *et al.*, 2000), morphological mapping at 1/1000^e scale in 1995, 1999 and 2001, installation of a heated

rain gauge (1994) and a climatic station (1996), preliminary geophysical prospecting by seismic refraction and electric resistivity in 1996. A geophysical and geotechnical investigation combined with a photogrammetric analysis was initiated in 1996 in order to determine the internal 3-D structure of the accumulated mass. Our main concern on this complex site was to obtain a maximum of information from different sources and then to compare them (Maquaire *et al.*, 2001). The classic techniques of punctual prospection by geotechnical drilling require an interpolation which is sometimes dangerous and we could not obtain a reliable picture of the structure without considerably increasing the number of drillings because of the heterogeneity and the extremely variable thickness of the earthflow both laterally and upto downstream. This increase in the number of investigation points was limited by the expense, particularly on this rather inaccessible site, which involved expensive helicopter transport for the heavy equipment which was needed to drill deep into the accumulated mass. It would not have been possible to reach a useful depth for investigation using light, low-performance equipment which a man could carry on his back. For these reasons we used geophysical investigation methods in addition to geotechnics. The investigations were carried out throughout five cross-sections, the location of which was guided by the specific morphologic features described earlier. Five pairs of aerial photographs were analysed by detailed photogrammetry (Fig. 2b, 2c, Weber and Herrmann, 2000).

Other investigations were carried out in order to analyse the hydro-mechanical properties of the earthflow: an on-going survey of surface movements by high-precision GPS (Malet *et al.*, 2000; Malet *et al.*, 2002); the installation of an extensometric device (Malet *et al.*, 2002); the installation of a water balance station to monitor pressure potentials; the installation of TDR-Trime tubes to monitor the soil moisture over depth; the installation three limnigraph recorders and a third rainfall gauge; experiments of rainfall simulations to identify the respective balance of infiltration or runoff water, depending on soil surface characteristics (Malet *et al.*, 2003b).

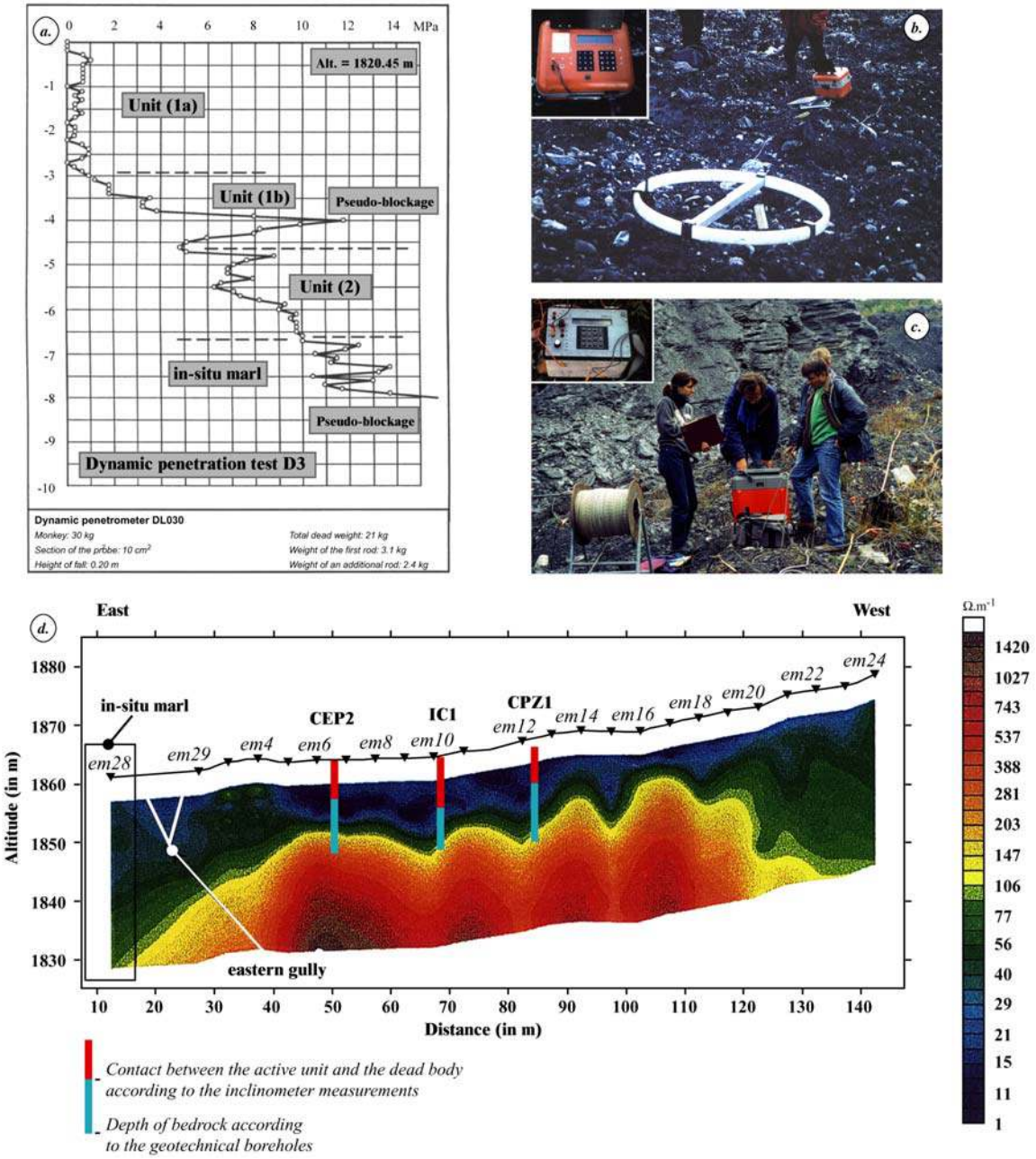

Figure 3. Geotechnical and geophysical investigation of the earthflow. (a): Example of a representative dynamic penetration test, (b): Time-Domain-Electro-Magnetism prospection, (c): eletric resistivity prospection, (d): 1-D interpretation of the TDEM soundings pairs on the cross-section C (after Schmutz, 2001) and results of the geotechnical interpretation.

3.3 *Principle retained to define the geometry and the internal structure of the earthflow.*

It was impossible for engines to access the site (muddy areas which would not bear them, gullies to cross), so light investigation tools (Fig. 3a) were used (dynamic penetrometer, percussion drilling) in addition to heavier tools. Inclinometric tubes and piezometers were installed and piezometric tests and water tests were carried out. A NUZI drill (100ch) was transported by helicopter and six deep drillings were carried out (with a core-sampling drill and five destructive drillings) on two flat zones in the upstream area of the flow (cross-sections 1 and C). The additional drillings were carried out with a heavy DL030 dynamic penetrometer (30 kg) and a percussion drilling device with gouges of from 30 to 100 mm enabling us to take intact or reworked samples to a depth of the order of 8-9 m. The general principle retained was to spread and correlate the various results obtained at a few points, then to extend the prospection using tools which were easier to handle, such as the dynamic penetrometer, the percussion drilling device and geophysical drillings (Syscal, Time-Domain Electro-Magnetism, electric prospection, seismic refraction, Fig. 3b, 3c).

The geophysical results are not given in detail here (Fig. 3d, on this subject see Schmutz *et al.*, 2000; Schmutz, 2001); however, we would like to discuss the geotechnical investigation. The results obtained from the various investigation techniques do not call for particular comment; they seem to be in line with their respective domains of validity. Nevertheless we would like to comment particularly on the results obtained by penetrometry in these formations and for places which are saturated. The dynamic penetrometers limited our investigations to a maximum depth of 9.50 m, in particular because of the development of lateral friction in the passage of the unstable and imbibed layers. The presence of many blocks of relatively unstructured moraine or marl within the mass also inhibited our investigations, as the drill could not penetrate these highly resistant materials. Finally, the presence of moraine pebbles or pieces of calcite within a less resistant layer gave rise to localised peaks (pseudo-blockages) on the penetrograms. In the *in-situ* marls (or in a block of mark buried in the earthflow) the resistance of the rod (Q_d) increases progressively, reaching values close to 25 MPa or more when the paleotopography was reached. Sometimes it was possible to force the penetration and then to continue the test within a less resistant layer. The D3 penetrogram clearly illustrates the major problem of pseudo-blockage, which could have been resolved in part by using a heavier drill. As the interpretation of tests could be difficult (blind testing) we were able to calibrate the resistance variations by means of several drillings, by digging ditches and by pressiometer tests. The shape of the penetration curves, even more than the crude rod resistance values $Q_{d,}$, is the discriminating factor which enables us to interpret the various layers. We were able to recognize three layers in the flow on most of the 178 penetrograms and these agree with the possible jumps in resistance (break in the curves, progressive transition).

4 STRUCTURE, GEOTECHNICS, HYDROLOGY AND KINEMATICS OF THE EARTHFLOW

4.1 *Internal structure of the earthflow*

Cross-correlation of all information available through a distributed database (geotechnical investigation, in-depth displacements by inclinometers, geophysical prospecting, photogrammetry) has allowed to build a 3-D geotechnical and hydrological model of the earthflow. The paleotopography comprised a series of crest quasi-intact in the accumulation zone. Some emerge over the earthflow on the B cross-section; others are intact to few metres under the surface. The earthflow presents a maximum thickness in the axis of the main gully of the 1956 torrential basin. It reaches a maximum of 20 m in the eastern part of cross-section C. Thereafter the thickness diminishes progressively towards the downstream area (8 to 9 m along the E cross-section, a few metres at the foot of the earthflow). The uncertainty of the thickness is minimal on the B and E profiles. However, the position of the substratum in the ablation zone is still uncertain because of the many pseudo-blockages in the penetration tests on cross-section A (blocks of moraine and many blocks and panels of structured marl). The penetration tests realized in the downstream part of the earthflow reach deeper depths. This means, firstly, that we have a smaller number of moraine blocks and secondly, a greater fragmentation of marly blocks within the reworked formation (Flageollet *et al.*, 2000).

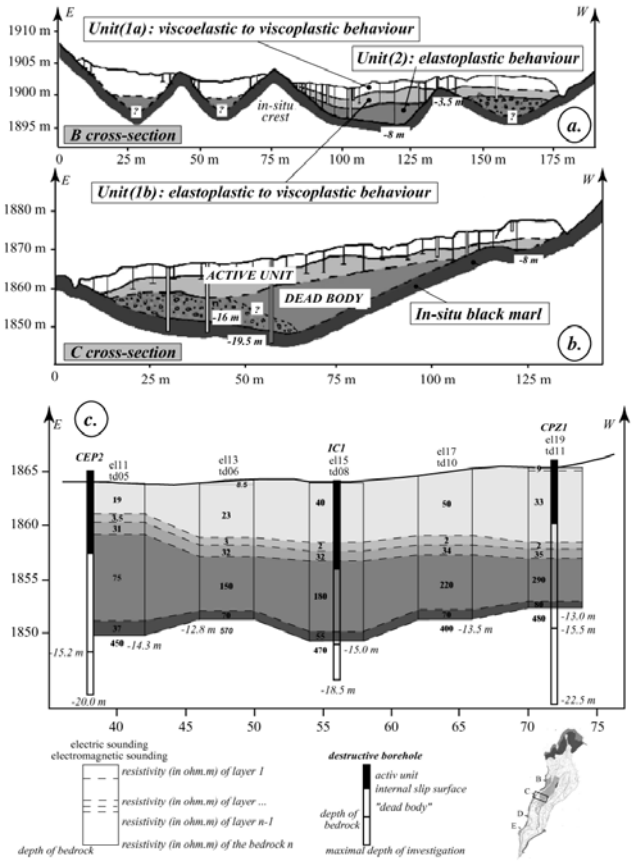

Figure 4. Geological structure of the earthflow. (a), (b):Geotechnical strucure on the B and C cross-sections, (c): Geophysical structure derived from a joint interpretation of electrical and TDEM soundings pairs (after Schmutz *et al.*, 2000).

The earthflow constitutes a heterogenous tongue with a high silty-sandy matrix mixed with morainic debris. In the accumulation zone (cross-sections B to E) three 'geotechnical' layers can be identified, based on the criteria of resistance, contrasts in the nature of materials and deformations and shearing of inclinometric and piezometric tubes. The read will find a detailed analysis of the mechanical characteristics of the materials in Maquaire *et al.* (in press). The vertical structure of the earthflow comprises (Fig. 4a, 4b):

- a thick superficial unit of 5 to 9 m (Q_d < 10 MPa, E_M < 15 Mpa, velocity greater than 5 m.year^{-1}). A shear surface has been identified at a depth of the order of 5 m on cross-section B and 8 m deep on cross-section C. This active unit can be sub-divided into two sub-units (1a and 1b), depending on the shape of the paleotopography and the seasonal position of the groundwater table;
- a deep unit with a maximum thickness of 10 m on cross-section C and 5-6 m on the western part of cross-section B. On the basis of inclinometric measurements and pressiometric tests (E_M > 15 Mpa, Pl > 4 Mpa), this unit is regarded as impermeable, very compacted with very little displacement or

stable as a 'dead body', as was identified at La Valette (Colas and Locat, 1993) or on the Slumgullion earthflow (Varnes and Savage, 1996).

If the geophysics indicates the same succession of layers (Schmutz *et al.*, 1999; Schmutz, 2000), the joint electric-TDEM interpretation (Fig. 4c) enabled us to demonstrate a thin, undetected transition zone (0.7-0.9 m) by geotechnical prospection (Schmutz *et al.*, 2001). This zone is the most highly conductive with resistivities which showed little contrast (2-3 Ω.m) and anisotropic factors from 0.35 to 1.0. These resistivity figures correspond to those present in samples of pure water. Furthermore the measurements were not disturbed by any provoked polarisation effect due to metallic or clay minerals. This being so this horizon must be saturated and would correspond to a shear surface between the active unit and the stabilized mass.

This compartmentalization in connection with gullies and crests is also evident because of the surface displacement measures (Malet *et al.*, 2002; Malet and Maquaire, 2003). The hydrodynamic and mechanical behaviour of the compartments varies with the seasons and the climatic conditions (Flageollet *et al.*, 2000; Malet *et al.*, 2002).

4.2 *Hydrological behaviour of the earthflow: rainfall-ground water table relation*

In the following, the hydro-climatic time series (rain, either liquid or solid, temperature, net radiation, soil water content, soil suction, pressure head, ground water level) over the period 1996-2001 and the results of an extended hydrological investigation are used. Around fifty open standpipe piezometers, filtered at different levels, have been installed at the five cross-sections since 1996. The significant dynamic of the flow involves the renewal of the piezometric dispositive every year.

4.2.1 *Aquifer geometry and hydrodynamical parameters*

The hydrological system has been determined according to geometrical (depth and thickness of the earthflow) and hydrodynamical parameters. The geometry of the hydrogeological system is identified by two static surfaces, the topography (DTM) and the bottom of the aquifer, and a dynamic one, the water table. The eastward and westward streams are considered as the lateral boundaries of the landslide system (Fig. 1h). The thickness of the aquifer (by crossing the data from the piezometric stations and according to transmissitivity calculations) reaches an average of 7-8 m on cross-sections A and C, 4 m on cross-sections B, D and E. We observe subsurface water fluxes between -0.5 and -1.5 m upstream of the earthflow (cross-sections A, B, C) and in the axis of the earthflow which is also the most active zone. Deeper water levels were observed around -2.5 m to -3.5 m in the western parts of the B and C cross-sections, in relation to the stream draining the ground water table. Moreover, the depth of the highest position of the water table slowly decreases from the B cross-section (-0.20 m) to the E cross-section (-0.80 m).

All matrix samples have a high content of silt and clay (25-40%, Maquaire *et al.*, in press) and the textural classes range from "silty clay" to "silty sand". The percentage of clay and silt fraction reaches 32-35%. Physical parameters such as specific gravity, dry unit weight, void ratio and porosity were determined on undisturbed samples. Bulk unit weight ranges from 16.6 to 17.1 $Mg.m^{-3}$ for a specific gravity ρ_s of 2.71. The natural water content varies considerably, ranging from 8 to 35%; the porosity ranges from 23 to 33% and the void ratio from 0.5 to 0.8. Atterberg limits classify the earthflow formation as inorganic clays of low plasticity (Ip = 11 to 19). The liquid limits range from 32% to 34%.

The hydrodynamical parameters (hydraulic conductivity, retention capacity, kinematic porosity) are very difficult to identify in such anisotropic system. A single point value (i.e., in a piezometric station or in a sample) can be calculated but the extension of the information to the whole area may be uncertain. Therefore, the sampling strategy consisted in identifying hydrogeomorphologic units on the basis of observed piezometric variations (Fig. 7a, 7b) and of morphological criteria such as the soil surface characteristics (Malet *et al.*, 2003b). Soil conductivities were extensively tested both in laboratory (constant and falling head permeameter) and *in-situ* (auger hole tests, tension disk infiltrometer, Beerkan tests, double ring infiltrometer tests) under pressure or suction. The variation in permeability with depth has been estimated by some sixty Lefranc tests (observation of the piezometric rise after draining the piezometers) and a Lugeon test on the *in-situ* marls. To estimate the lateral conductivity K_L, soil samples were taken horizontally at different depths, following the methodology proposed by Caris and Van Asch (1991). The matric suction-moisture content relationship was obtained through a sand and kaolin box apparatus for pressure heads between pF 1.0 and pF 2.7, and with a suction plate membrane apparatus for pF 3.6 and pF 4.2. The maximum water storage was derived from these pF curves on more than 250 samples.

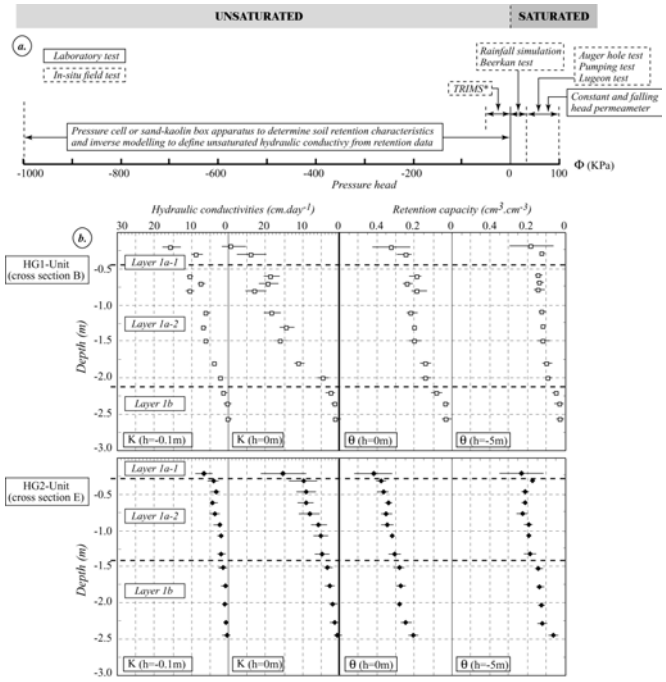

Figure 5. Hydrodynamical properties of the earthflow. (a): Hydrolocical experiments performed to study the hydrodynamical behaviour of the material in both unsaturated ans saturated conditions, (b): Variation of conductivity and retention capacity over depth with special reference to the units HG1 and HG2.

The observed hydrological behaviour is in accordance with the texture of the soils. The conductivity values classify the material as semi-permeable (Fig. 5b). The conductivity values of the subsoil vary according to the soil surface characteristics (Malet *et al.*, 2003b) and the presence of fissures from 10^{-4} $m.s^{-1}$ to 10^{-8} $m.s^{-1}$. The conductivity values obtained *in-situ* are higher, though more scattered than those in the laboratory tests. This can mainly be explained by the facts that: (1) the void ratio increase which should produce an increase in permeability is probably compensated by the spatial obliteration of the fissures which constitute a preferential water flow path; (2) the soil surface characteristics (size of the embedded elements and crusting) govern the conductivity near saturation (Malet *et al.*, 2003b) and (3) *in-situ* tests are marked by 3-D effects. The retention values are high and range between 0.17 and 0.42 cm^3/cm^3. The matric suction-moisture content relationship is well represented, either by a complex Van Genuchten (1980) model or by a simpler Farrel and Larson model (1972). These values agree with average results for similar black marl soils in the literature (Caris and Van Asch, 1991; Mulder and Van Asch, 1988a; Mulder and Van

Asch, 1988b; Antoine *et al.*, 1995; Van Asch, 1997; Van Asch and Buma, 1997). The auger hole tests show a decrease in the permeability with depth, connected with the increasing compaction of the materials, with values of up to 10 $m.s^{-1}$ between -1 m and -2 m, up to 10^{-11} $m.s^{-1}$ in the dead body of the earthflow. A fairly high seasonal variation in permeability can be identified between May and October. Furthermore the Lugeon test carried out *in-situ* indicates a permeability of 10^{-9} $m.s^{-1}$. This allows us to state that the whole 'dead body' reworked material and the underlying *in-situ* intact material can be regarded as impermeable.

The average transmissitivity of the aquifer, calculated following twenty one piezometric rises on the B and E cross-sections with the analytical solution of Théis and the logarithmic approximation of Jacobs (Théis, 1941; Freeze and Cherry, 1979), is as high as 10^{-3} $m^2.s^{-1}$. These calculations enabled us to estimate the storage coefficient (i.e. effective porosity) of the aquifer, which is very low (0.15 ± 0.04). The effective porosity estimated using the Théis equation (15%) is confirmed by the laboratory porosimetry measurements in mercury, which give a kinematic porosity from 17 to 23% for the reworked marls.

4.2.2 *Mass balance factors of the hydrological system*

Inputs (rainfall and snowfall) and outputs (surface water, evaporation) of the saturated zone represent the mass balance of the system. The yearly average precipitation is usually approximately 750 to 900 mm (with around 200 to 250 mm as snowfall), but the maximum daily or monthly value can vary and produce significant groundwater fluctuations (Flageollet *et al.*, 1999). A monthly value of 150 to 200 mm can occur especially in April, May, October or November. Three rain gauges installed in a 5-square kilometre area around the landslide allow to quantify rainfall variability. A climatic station allows to estimate the reference potential evapotranspiration according to Penman's equation and records Snow Water Equivalent. Finally snow is considered because it is the main mode of precipitation during winter. A snow depth sensor is installed since 1999 on the site, at 2000 m a.s.l.

No springs are visible on the flanks of the earthflow. The discharge were measured temporarily in the midstream section of the main drainage axes of the landslide, under different climatic conditions; The field observations showed very high peaks in stream discharge, during a period of medium-high rainfall, and no lag time with precipitation was measured. Unfortunately, the hydrograph could not be evaluated. More information is needed to reproduce quantitatively this hydrological aspect of the system. Three continuous piezometers were installed from 1997 onward (soil suction probes, soil moisture probes) to study in detail the infiltration process in the unsaturated zone.

4.2.3 *Qualitative inferences from field data: analysis of ground-water flow*

The earthflow is characterized by high groundwater levels. Figure 6 shows an example of the rainfall – groundwater table relationships for the year 1998 in the lower part of the earthflow. The piezometric fluctuations are correlated with rainfall (Malet *et al.*, 2002). The kinematics follows a seasonal trend with two acceleration periods in spring and in autumn and two deceleration periods (corresponding to hydrological drainage periods) in summer and in winter when snow covers the flow. The analysis of the piezometric behaviour shows high pore pressure variations (up to 20-25 kPa corresponding to an average fluctuation of the groundwater level of about 2.5 m) with sudden recharge following the snowmelt. Pore pressures may remain high for a long time due to the medium permeability of the reworked marls, and the presence of the impermeable dead body at the bottom. Groundwater table fluctuations follow strictly the same trend all over the earthflow, but the relative position of the water level depends on local conditions. Water levels fluctuations of different intensity are related to the changes of the permeability and geometry of the earthflow.

Daily precipitation in relation to the daily groundwater fluctuations has been analysed statistically (auto-correlation functions, cross-association and correlation techniques) on four automatic piezometric stations over the period 1999-2001, and on twenty one piezometric stations between June and October 1996 with daily manual recordings (Velcin, 1997).

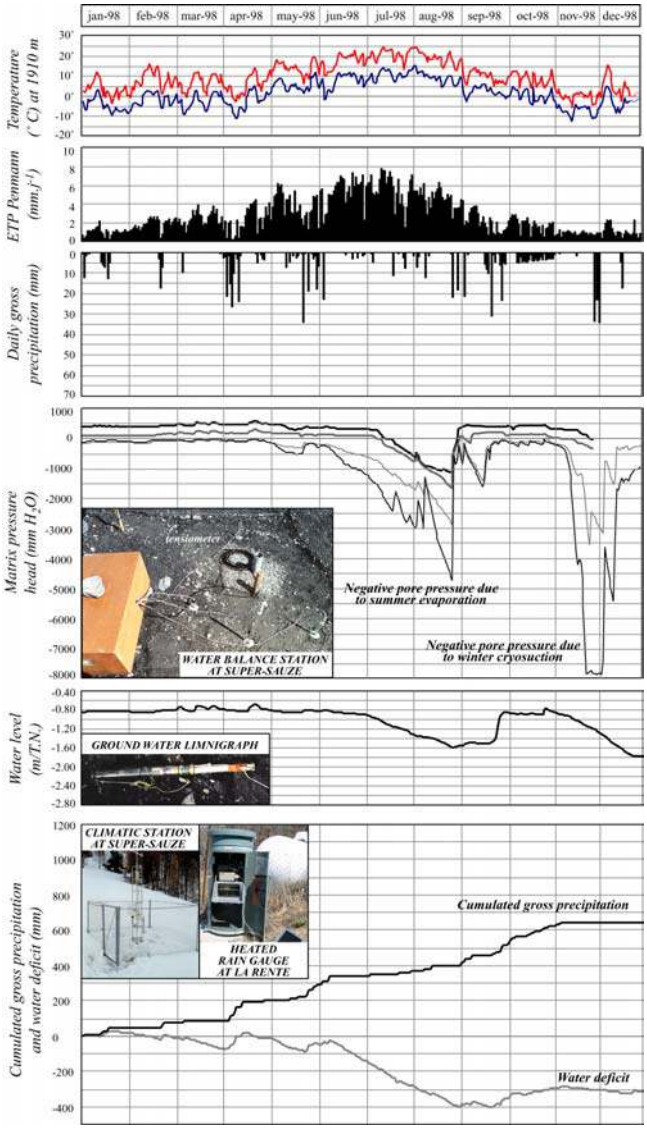

Figure 6. Example of climatic, soil and groundwater time series over the year 1998, and associated sensors.

Figure 7c shows an example of the autocorrelation function of the ground water level fluctuations of the four pore water pressure sensors used. The autocorrelation functions of BV5 and E2 show a high autocorrelation value (> 0.3) for time lags up to 10 days. The fact that these piezometric stations have long gradual rising and falling stages is the explanation for this correlation. They also correspond to the less active part of the earthflow. CV3 and in particular BV16 show less much autocorrelation. These piezometric stations experience short-term fluctuations and are more influenced by external factors (fissure density) than by system memory.

These analyses confirm the hydro-geomorphological units identified previously (see section 4.2.1). Considering autocorrelation functions of CV3 and BV16 similar, three units can be identified (Fig. 7a):

- the *HG1 unit*, featuring very rapid piezometric responses (< 1 hour), a significant fluctuation (up to + 0.4 to 0.5 m) and relatively rapid drainage (3-5 hours);

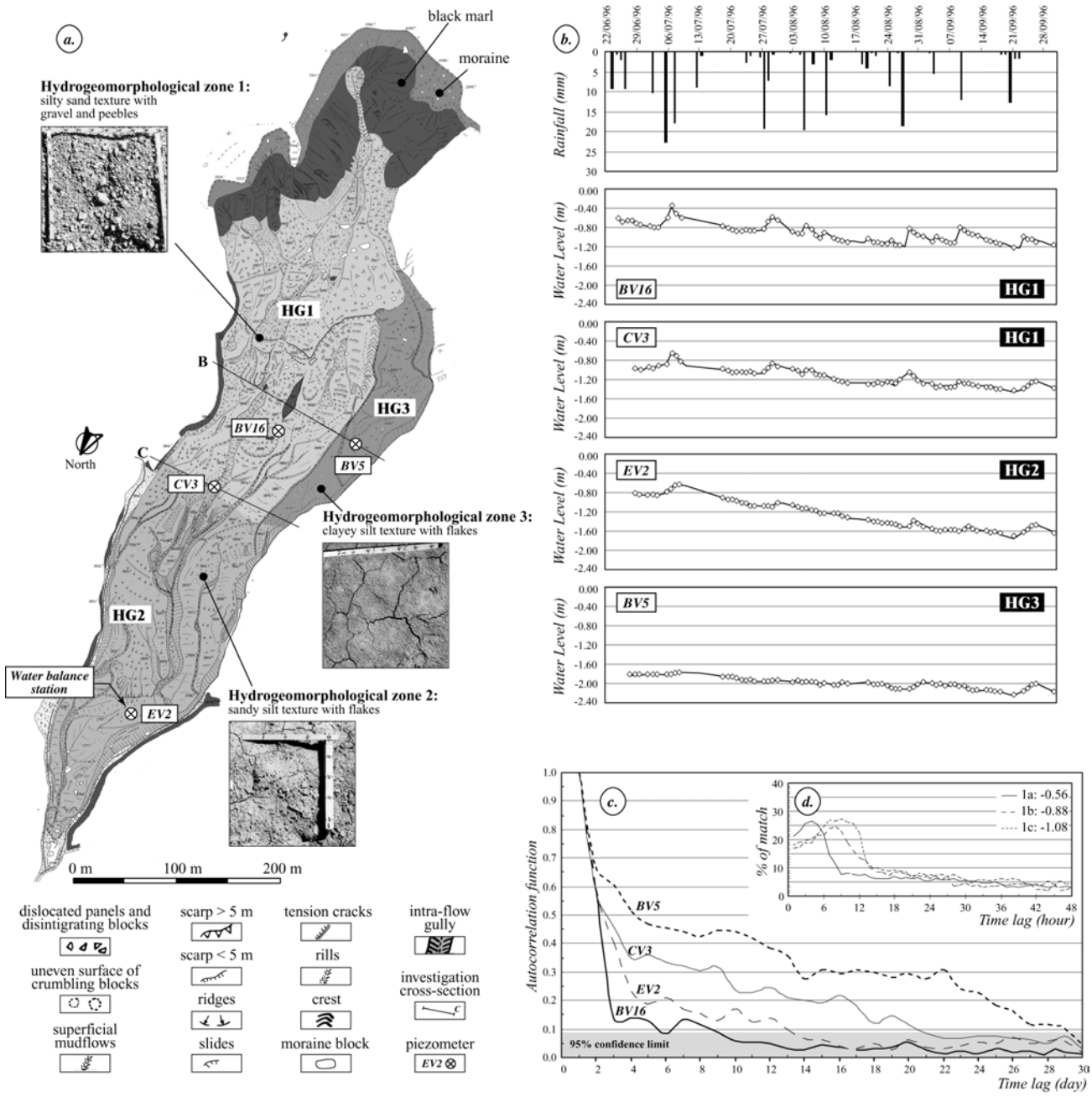

Figure 7. Hydrogeomorphological units of the earthflow. (a): Boundaries of the hydrogeomorphological units and representative soil surface characteristics, (b): Characteristic groundwater table variation within each units defined through punctual daily measurements over a period of 3 months on thirty piezometers, (c): Autocorrelation functions for ground water level fluctuations of four monitoring locations, (d): Cross-association results of soil suction fluctuations for three monitoring depths.

- the *HG2 unit*, with rapid piezometric responses (2-3 hours), an average fluctuation (+ 0.05 to + 0.3m) and rapid drainage (12-24 hours);
- the *HG3 unit*, with slow piezometric responses (> 5 hours), low fluctuation (centimetric) and slow drainage (> 24 hours).

A factorial analysis of correspondences enabled us to establish a typology of effective rainfall (i.e. which recharges the groundwater table) at the event scale. It can be stated that:

- almost all rainfall lasting less than ten minutes involve few or low groundwater rises (< 0.05 m);
- groundwater rises greater than 0.1 m follow rainfalls of more than 10 mm;
- the most significant groundwater rises (>0.4 m) always follow the melting of a fairly heavy snow cover.

It would also appear that the majority of rises occur when the groundwater table is in a high position of around –1 m, showing the influence of the unsaturated zone.

The infiltration in the unsaturated zone can be studied more in detail through the analysis of the soil moisture variations, and the short-term variation of soil suctions. These fluctuations are representative of the HG2 unit (Fig. 6). On an annual basis, the amplitude of soil suctions varies between saturation and in average + 150 hPa. In specific situations, soil suction can reach more than 400 hPa, such as in July 1998, or even 800 hPa when the soil freezes (example of November 1998).

In this unit we notice the quickness of the water transport to depth, as there is an immediate drop in pressure potentials after rainfall. As these data relate to low hydraulic conductivities of the soil matrix they are connected to fissures and to macropores

fluxes. We also notice above all that after rainfall saturation always remains local up to around 0.5 m. and temporary (1/4 h to 2 h maximum.). Over the period 1997-2001 the topsoil (0-0.75 m) was never saturated in the HG2 unit.

The cross-association between (effective) precipitation and soil moisture changes was performed to determine the time delay in the infiltration process (Fig. 7d). The precipitation and soil moisture data are on a hourly basis, which impels the matching to be performed on the same time scale. It is recognised that this time resolution is high for the infiltration process in semi-permeable soil. All soil moisture time series give similar results for the cross-association analyses. The results show a time lag of maximum four hours for the upper part of the topsoil (-0.56 m), and of maximum 9 to 10 hours for the lower part of the topsoil (between -0.88 m and -1.08 m). The percentage of matches decreases between time lag 4 to 9 for the upper part of the topsoil, and between time lag 9 to 15 for the lower part of the topsoil. The deeper installed soil moisture probes have a slightly larger time lag than the shallow soil moisture probes. Nevertheless, the higher matching percentage is the same between the shallow and the deeper soil moisture. The results described above show that the unsaturated zone (to 0.75 m depth) reacts generally within 4 hours on a rain event. The cross-association technique was also used to determine the time delay between (effective) precipitation and ground water level reaction, taking into account the same piezometric stations as for the autocorrelation analysis. From these results, it can be assumed that recharge of the groundwater table is mainly controlled by matrix Darcian flow in the wettest periods of the year (spring) and by a mix of matrix flow and fissure flow the rest of the year.

4.3 *Kinematical behaviour of the earthflow: ground water table-displacement relation*

Five years (1997-2001) of continuous displacements and pore water pressures monitoring have demonstrated that the earthflow accelerations are totally controlled by hydro-climatic conditions and generally the result of the undrained reactivation of the reworked material; the induced displacements being characterised by a high variable rate (Malet and Maquaire, 2003). Displacements along the earthflows correspond to the line of greatest slope. The general direction of the displacements is facing N-10° on the cross-sections A, B, C and E and N-340° on the cross-section D and on the toe of the flow, underlining the influence of the paleotopography on the dynamics of the flow. The spatial variability of the displacements along the transverse cross-sections suggest that the landslide body acts as a deformable medium whose behaviour depends on shape of the covered gully, on the position of the groundwater table in each compartment, and on the local induced strain field.

Two thresholds of pore pressures trigger the acceleration of the movement; above it, the velocity increases non-linearly. The "spring movements" are initiated as soon as the water level ranges between -0.8 and -0.7 m below the ground surface; the "autumn movements" are triggered by a higher threshold value (between -0.6 and -0.5 m below the ground surface). This higher level is probably explained by strength regain due to an increase in undrained cohesion by consolidation in summer (Salt, 1988; Van Asch and Bogaard, 1998).

It appears therefore that rainfall is the main triggering factor of the earthflow mobility, producing an intermittent and delayed recharge of the groundwater. The long-term behaviour is characterized by continuous movements with a seasonal trend. The earthflows may be active for decades or more as is justified by the very low Factor of Safety of the landslide body (mean ϕ'_r=20°, mean slope angle β=25°) very often below 1 (Maquaire *et al.*, in press). Once a threshold pore pressure distribution is attained, the rate of movement increases. Also, while pore pressures decrease, velocity decreases too, but no stop of the movement is observed. This may be explained considering that both the residual strength parameters and the applied shear stresses are constant with time, as suggested by Picarelli *et al.* (1999) for clay shale earthflows in the Southern Apennines.

Excess pore pressures are therefore only related to infiltration (Malet *et al.*, in press). This scheme corresponds to the seasonal long-term dynamics of the earthflow. It can be well represented by viscous analytical laws (Malet and Maquaire, 2003). Under exceptional hydroclimatic conditions (conjunction of snowmelt, thawing, and rainfall), short-term dynamics of the earthflow involves the emergence of the groundwater table at the topographic surface, the evolution of the rheology and the initiation of debris-flows (Malet *et al.*, 2003a).

5 CONCEPT FOR THE HYDROLOGICAL BEHAVIOUR OF THE EARTHFLOW AND MODEL IMPLEMENTATION

5.1 *The hydrological concept*

The following conceptual hydrological model can be proposed:

- above a certain threshold level (0.6-0.8m in the HG1 unit, 0.8-1m in the HG2 unit), groundwater fluctuations are invariably rapid (less than a few hours), moderate (0.1 to 0.4m) and of short duration (within days), following liquid rainfall. Peaks following snowmelt have a longer duration;
- the fall of the groundwater below this level strongly depends on the season, with much faster drainage in summer;
- the hydrological regime is influenced by two important recharge events, one at the end of spring and one at the beginning of autumn;
- no deep alimentation within the landslide body has been established.

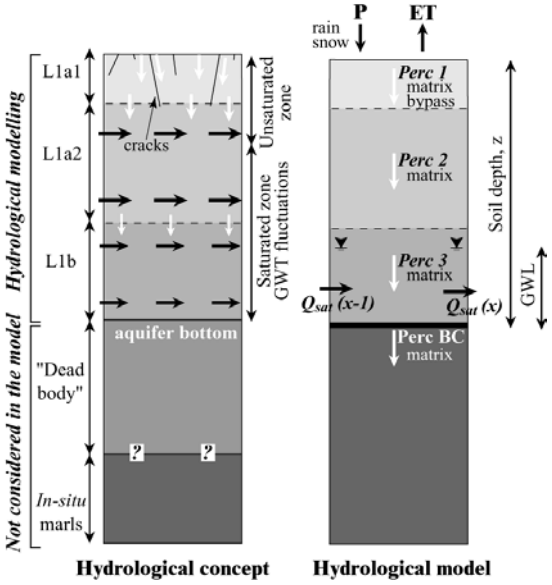

Figure 8. Hydrological concept of the earthflow and implemented hydrological model.

Therefore, the rapid piezometric responses are attributed to an infiltration process through a superficial (0.3-1m) system of interconnected cracks (swell/shrink fissures and kinematic cracks). The depth of this crack system correspond mainly to the mean contact between the unsaturated and saturated zones and works as a fast flowpath from the ground surface to the water table. This contribution is not the same for all the measurements stations due to differences in cracks density and soil surface characteristics, so it can be considered as one of the main reason for the different rates of groundwater rise.

The failure of many smaller summer rainfall events to produce any groundwater rise suggest a water deficit in the matrix of the first layer caused by evaporation. The relation between precipitation and piezometric variations could not be related only to vertical infiltration, but also lateral infiltration could play an important role. These considerations are schematised into the

following hydrological concept in three layers. A layer with a continuous permeable crack system (L1a1) overlies two layers marked by different matrix conductivity values (L1a2, L1b) due to compaction. The groundwater table is mainly located in the L1b and L1a2 layers. The "dead body" is impervious and thus not considered in the hydrological model. A similar behaviour has also been observed in the Alverà landslide (Angeli *et al.*, 1998; Bonomi and Cavallin, 1999).

This hydrological concept was incorporated into a numerical model (Fig. 9a) by adaptating the spatially-distributed physically-based model STARWARS (*Storage and Redistribution of Water on Agricultural and Revegetated Slopes*, Van Beek, 2002). A compromise between the complex topography, the spatial distribution of soil properties, the temporal resolution of the meteorological and hydrological records has been found to fix the model spatial resolution (2m) and the temporal timesteps (6 hours).

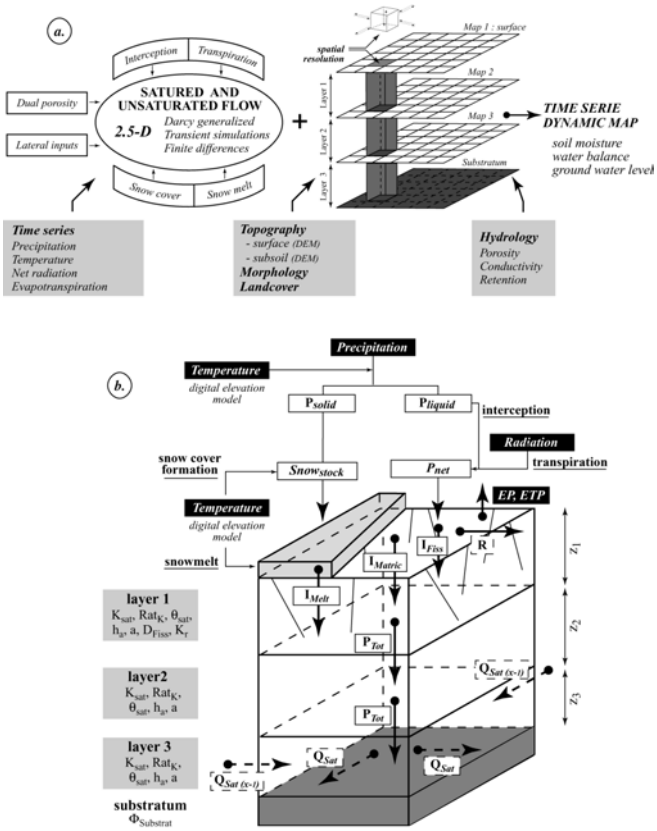

Figure 9. Architecture of the STARWARS model. (a): Modular architecture of the model (core, module) and schematic representation of the model implementation in the *PcRaster GIS* package, (b): 2.5-representation of the earthflow by combination of maps and relation between the cell attributes.

The model consists of three permeable reservoirs (the three layers) and the bedrock is assumed impervious. Therefore the response of the groundwater is imposed on a generated water level over this impervious lithological boundary that restricts the direct loss of soil moisture into the bedrock.

Antecedent soil moisture condition in the different layers, infiltration *Inf*, evaporation *Ep*, percolation in the unsaturated zone *Perc* and saturated lateral flow Q_{sat} are taken into account. Within one timestep, water is added to the saturated storage by the percolation from the unsaturated zone and from bypass flow in the fissures if any occurred. The saturated storage is diminished by the loss over the impervious bedrock and by evaporation, only substantial when the groundwater is close to the surface.

5.2 *The hydrological model STARWARS*

The model describes the saturated and the unsaturated transient flow, in the vertical and lateral directions, assuming freely drainable water (Fig. 9a, 9b). Percolation is limited to gravitational vertical flow and defined as a function of the elevation potential only, neglecting the matrix potential for the flow in the unsaturated zone. Over the saturated zone, the piezometric head defines the lateral flow. All storage and fluxes, given in units of waterslice (m), are expressed by the relative degree of saturation θ_E of each layer. For each model layer *z*, the vertical unsaturated matric flow (the percolation) is controlled by the unsaturated hydraulic conductivity $K(\theta_E)$. The mathematical formulation of Farrel and Larson (1972) of the Soil Water Retention Curves, combined to the capillary analogy of Millington and Quirk (1961), and the K_{sat} values are used for the calculation of the unsaturated conductivity. Percolation is thus proportional to the travel time of soil moisture over the unsaturated zone, and is deducted directly from the drainable storage in the unsaturated zone. It is then used to recalculate the resulting degree of saturation for the next timestep. As a clear dual porosity network exists in the upper layer, bypass flow through the fissure is also considered. A fraction of the rainfall excess *DirRepl* is transferred directly in depth within one timestep by bypass flow.

The lateral outflow Q_{sat} over the saturated zone is controlled by the piezometric gradient *i*, defined by the absolute elevation of the phreatic surface. A Local Drainage Direction map *LDD* of the groundwater height is derived to identify the drainage direction. The piezometric gradient *i* is given by the difference in elevation over the slope parallel distance. Along the *LDD*, the lateral outflow travels with the apparent velocity of the saturated lateral conductivity K_L, which is a fraction of the vertical K_V. Then, for each cell, the storage of the saturated zone is balanced for the outgoing and incoming fluxes.

The generation of the groundwater is simulated by imposing boundary conditions. The lower boundary conditions are state-controlled and are specified as fixed values for the matric suction *PsiBC*. It is a suitable parameter for model calibration. The upper boundary conditions are flux-controlled and concern the meteorological inputs at the surface (rainfall, temperature, evaporation, net radiation). At the surface, a simple infiltration module is used assuming that the maximum infiltration capacity is defined as a ratio of the saturated conductivity of the top layer. The infiltration is only limited if the net rainfall exceeds it.

A snow cover and snowmelt module is incorporated as preprocessor in the hydrological model. It is based on four components: (1) an input transformation, correcting for the representativeness of climatic inputs (precipitation, temperature and radiation) with respect to altitude, (2) a surface melt component using a simple excess temperature mechanisms as a substitute for a full energy budget controlled melt formulation, (3) a snowpack storage mechanism, controlling how surface melt is retained within the pack, and (4) a drainage term defining the release of water from the pack and formulated as an integrated part of (3). The SNOWPACK/MELT model employs representations particularly suited to South Alps conditions. A temperature threshold (*Ts*) is used to discriminate rainfall (*R*) and snowfall (*P*). A typical value for *Ts* in South Alps conditions is 1.5°C. A critical temperature (*Tm*) above which melt (*M*) occurs and a melt factor (*f*) are used to govern the melt equation. A *Tm* value of 0°C is taken. An extension to incorporate wind speed may be important for mountain conditions (Singh *et al.*, 1997) but the added level of complexity has not been incorporated in the current implementation of the model.

The model components use the embedded meta-language of the PcRaster GIS package (Wesseling *et al.*, 1996). Based on available knowledge, the model uses measured distributed values for the parameter values, where each layer is represented by a map. Implementation in a GIS-environment has several advantages. First of all, if based on a high resolution DEM, the effect of topography can readily be incorporated and the GIS offers the

direct use of the available routing functions to define flow paths for saturated and unsaturated flow in each layer. Secondly, it is possible to include the spatial variation (lateral and vertical) of the hydrological parameters. This approach provides a unified theoretical description of most of the water fluxes observed within a landslide; we can therefore use the diffusivity equation which combines Darcy's law with the water conservation equation to model the fluxes in the saturated zone, and we can use Richards' equation combining the generalised Darcy's law equation with the water conservation equation in the unsaturated zone.

6 MODEL CALIBRATION AND VALIDATION.

6.1 *Model calibration*

The model formulation is defined *a priori* and calibration only consists of the optimisation of the model performance by adapting the hydrological parameters on the basis of field evidence. For calibration, the EV2 and BV16 piezometers were chosen. The model was calibrated over the period January-December 2000 and validated over the period January 2001-December 2001. In a first time, to test the model capabilities, some simple calculations were performed, assuming homogeneous mean characteristics for all the moving mass and no distributed parameters. These preliminary results are presented and discussed in the following section.

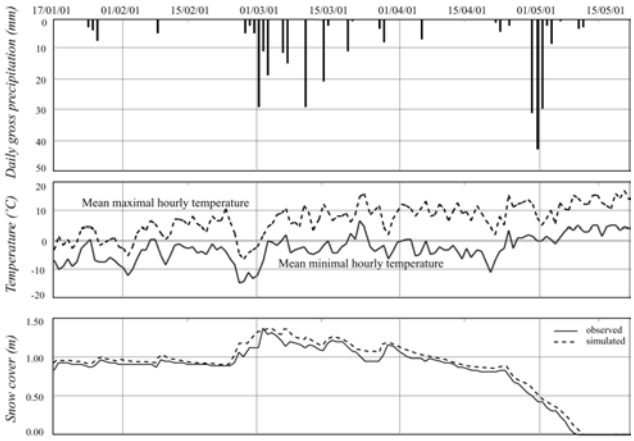

Figure 10. Calibration of the SNOWPACK/MELT model.

Table 1 gives an overview of the mean values and estimated ranges of parameters used in the hydrological simulations, and gives the calibrated parameters that produced the best calibration fit. In a first step, to produce initial distributed water level, soil moisture and snow thickness conditions, the model was run over a 25-years period using the meteorological data of Barcelonnette (1975-2000), and the average hydrological parameters measured in the field.

In a first stage, the SNOWPACK/MELT model parameters (a_r and m_Q) were calibrated separately using the continuous monitoring of the snow thickness between January and May 2000 (Fig. 10). The best calibration fit was found for a_r=0.28, m_Q=0.042, a snowing temperature of 2°C and a melting temperature of -0.5°C. These values are in accordance with the range given by the reference (1986). The runoff coefficient *RC*, which controls the direct contribution to waterlevel by bypass flow, was derived from rainfall simulation tests.

Figure 11 shows the simulation results for piezometers EV2 and BV16. The response pattern is reproduced very well; although some recorded peaks, especially for BV16, are underestimated or missed. This seems not so important as these very quick lasting high groundwater levels do not influence the kinematics behaviour of the earthflow (Malet *et al.*, 2002).

The drainage conditions and the range of groundwater levels fluctuations are well simulated; it demonstrates thus that the estimation of the evaporation parameters by the Penman formula is quite adequate.

At the opposite, the quickness of the important recharges (often in less than one day) is not simulated by the model; the duration of the simulated recharge spread out over several days. It is assumed that a distributed repartition of the parameters with higher conductivity values, porosity values and density of fissures in the upper part of the earthflow, will be helpful to explain this mismatch. Also the Snow Water Equivalent simulated during the melting of the snow cover is underestimated, as the density of the snow is not introduced in the model. Due to the importance of the drainage periods over the year, a specific calibration on the recharge events alone could also ameliorate the results.

The parameters listed in Table 1 were adjusted to come to the smallest Root Mean Square Error (RMSE) for the observed versus simulated time series. Two important aspects of a model are its performance after the calibration period, during the validation, and the choice of the fitting time series. In our case, the modelled time series can be optimised on the soil moisture variation in the topsoil (at 4 depths) or on the groundwater levels.

Table 2 shows the results of RMSE calculated for the calibration (2000) and validation (2001) period, as well as the ratio for the two periods. These calculations were executed by automatic iteration using the Marquardt-Levenberg algorithm implemented in the PEST software (Marquardt, 1963). Upper and lower boundaries conditions (± 50% of the minimal and maximal measured values) were fixed for each parameter.

Table 2 shows that the model performance is slightly higher with the soil moisture data set than with the ground water level. This is not surprising as the generation of the ground water table in the soil by downward percolation is controlled by the soil moisture balance in the topsoil. Calibration on the ground

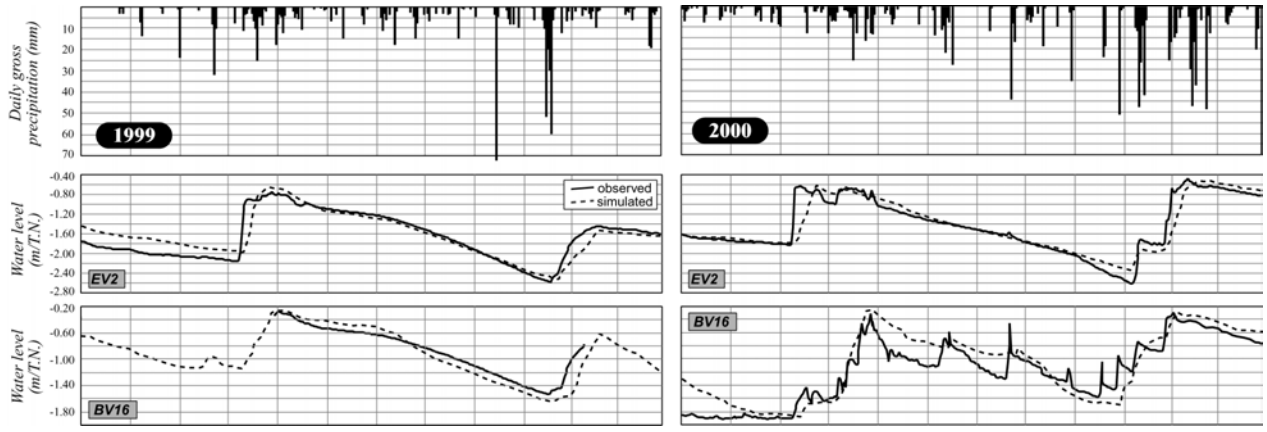

Figure 11. Observed and simulated groundwater levels over years 2000 and 2001 (year 2000 is the calibration period, year 2001 is the validation period).

Table 1. Overview of the field-measured parameters and of the fit parameters for the different model calibration tests.

Parameters	Description	Field measurements			Model input values
		Mean	Range	n	GWL
Kv_1 (cm.d^{-1}) *	Saturated vertical conductivity – layer 1a1	0.78	0.53 – 0.91	131	0.40
Kv_2 (cm.d^{-1}) *	Saturated vertical conductivity – layer 1a2	0.53	0.42 – 0.72	86	0.30
Kv_3 (cm.d^{-1}) *	Saturated vertical conductivity – layer 1b	0.47	0.35 – 0.52	47	0.30
Rat_K (–)	Ratio Lateral/Vertical conductivity	0.46	0.39 – 0.56	67	0.01
$ThetaSat_1$ (–) *	Porosity value – layer 1a1	0.43	0.36 – 0.49	142	0.38
$ThetaSat_2$ (–) *	Porosity value – layer 1a2	0.37	0.30 – 0.46	93	0.24
$ThetaSat_3$ (–) *	Porosity value – layer 1b	0.31	0.23 – 0.39	61	0.21
ha_1 (m) *	Air entry value – layer 1a1 (SWRC)	0.024	0.008 – 0.042	142	0.021
α_1 (–) *	Shape factor of the SWRC – layer 1a1	13.6	12.9 – 14.7	142	10.1
ha_2 (m) *	Air entry value – layer 1a2 (SWRC)	0.042	0.035 – 0.049	93	0.031
α_2 (–) *	Shape factor of the SWRC – layer 1a2	12.3	11.5 – 13.1	93	7.1
ha_3 (m) *	Air entry value – layer 1b (SWRC)	0.021	0.016 – 0.021	61	0.017
α_3 (–) *	Shape factor of the SWRC – layer 1b	13.2	12.3 – 13.7	61	10.0
a_r (cm.°C)	Restricted-degree day factor	–	0.20 – 0.25**	–	0.28
m_Q (cm.day^{-1}/W.m^2)	Conversion factor for energy flux density	–	0.05 – 0.033	–	0.42
DirRepl (–)	Density of fissures and macropores	0.07	0.01 – 0.15	233	0.04
RC (–) ***	Runoff coefficient	0.2	0.1 – 0.4	35	0.35
PsiBC (m)	Matric suction of infinite store under bedrock	-	–	-	2.98

*: index number refers to the layer related parameters; **: values given by Martinec and Rango (1986); *** estimated by rainfall simulation

Table 2. Validation results of the STARWARS model: GWL stands for fitting on the ground water levels time series at two piezometric stations, SM stands for the fitting on the topsoil soil moisture time series at four depths, RMSE stands for root mean squared error, Ratio stands for the ratio of RMSE of validation period over RMSE of the calibration period.

	Calibration: 1 calendar year	Validation	Ratio	Calibration: 1 hydrological year	Ratio	Calibration: drainage periods	Ratio	Calibration: recharge periods	Ratio
	RMSE [m]	RMSE [m]	Val/Cal	RMSE [m]	Val/Cal	RMSE [m]	Val/Cal	RMSE [m]	Val/Cal
GWL (2)	0.030	0.043	1.423	0.033	1.302	0.028	1.274	0.051	1.270
SM (4)	0.027	0.039	1.422	0.028	1.384	0.022	1.129	0.042	1.259

.

water levels necessitates some additional parameters to optimise. Moreover the optimisation performed on the drainage periods solely results in higher RMSEs. This result implies also that the soil moisture balance and the evaporation process are well represented by the model. At the opposite, the recharge periods are poorly represented. This can be explained by an underestimation of the fissure flow. Finally, results show that the model performance is generally poorer in the validation period. Longer training data sets should be used.

Table 1 shows the best-fit parameters resulting from the best optimisation (with the lower RMSE). Best-fit parameters are in the range of parameters estimated in the field. The porosities values *ThetaSat*, the ratio between lateral and vertical conductivity Rat_K, the SWRC parameters and the matrix suction of infinite store at the bedrock contact *PercBC*, which controls the loss of water in the 'dead body', have been found as the main sensitive parameters.

6.2 *Model sensitivity*

The sensitivity of the model to changes in parameterisation and in model geometry has been analysed by comparing the simulated hydrology of the earthflow for the year 1999. The total drainable storage was used as a general measure of the simulated hydrology. Starting with the same initial conditions (the average winter profile in moisture content) the response of the moisture content in the three layers and of the ground water levels has been modelled, with the input climatic data of 1999. The seven tested parameters are varied in consecutive model runs and the model outcome is compared to that for the reference parameterization. Only one parameter is perturbed in each run. The remnant parameters are kept at constant values. The model has been simplified by assuming no distributed parameters (only one hydrological unit). The parameter changes have been calculated by subtracting or adding 10%, 25%, 50%, 100% and 200% of the standard deviation to the mean parameter value. If the variability is unknown, an estimate has been used.

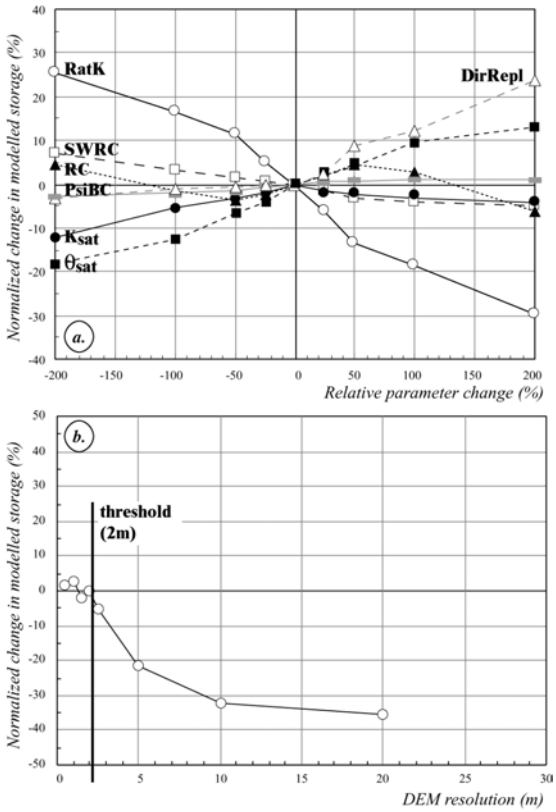

Figure 12. Sensitivity of the simulated hydrology, expressed as the change in total storage, to changes in seven model parameters (a) and DEM resolution (b).

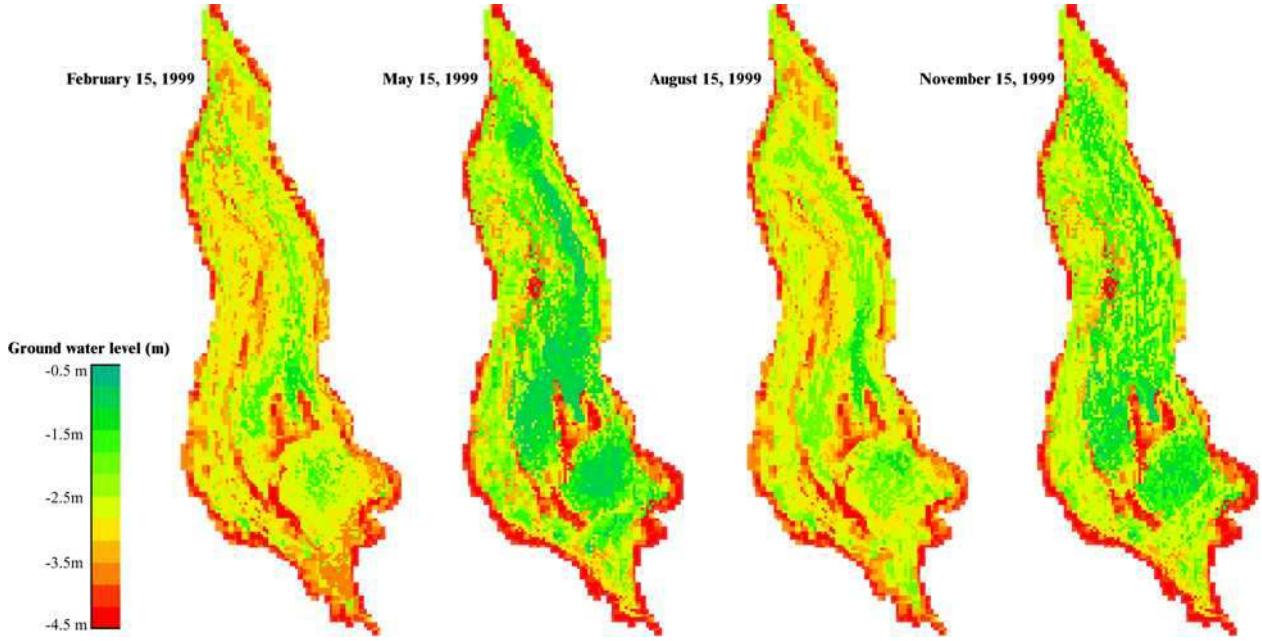

Figure 13. Distributed representation of the ground water levels fluctuations over time. One map is calculated at each time step (6 hours).

In Figure 12a, the normalized changes in modelled storage are given for the respective parameter increments. The hydrological model is the most sensitive to the ratio between the vertical and lateral saturated conductivity. A change by ± 25% of the ratio results in a deviation of more than 15% in the modelled storage. This ratio is therefore a suitable parameter for model calibration. Porosity and the density of cracks are the parameters with the second and third larger influences. This is not surprising as these two parameters control the soil moisture percolation in depth, and thus the overall infiltration process. The others parameters have less influence and behave in a less orderly manner. The deviations in drainable storage are less than 5%. Among these parameters, the characteristics of the soil water retention curves have the highest influence. In Figure 12b, the normalized changes in modelled storage are given for different simulations with different cell size (respectively 0.50 m, 1 m, 1.50 m, 2 m, 3 m, 5 m, 10 m and 20 m), by keeping all the other parameter values constant. DEM resolution has a high influence. Coarse resolution (larger than 5 m) results in an underestimation of more than 20% in the modelled storage. A threshold is clearly identified around 2 m. Below this threshold, integration of finer resolution does not deviate, neither ameliorate the model.

The results of simulations may be presented in distributed form (Fig. 13). This makes it possible, for example, to locate exactly the highest zones of water levels. In our case these zones are to be found upstream of the earthflow in the area which presents the highest velocities.

7 MODEL PREDICTION AND PRACTICAL USE

Once the model is validated on real observations, and when the model appears to give an accurate representation of the physical processes under consideration it can be applied to hypothetical cases. Two practical applications are presented below.

7.1 *Long-term behaviour of the flow: impact of environmental changes.*

The dynamic nature of this type of model enables us to test the influence of changes in climate or land use on the earthflow hydrological behaviour. These elements can help the expert responsible for defining a hazard level (thresholds for the appearance of phenomena, occurrence of high groundwater levels). Numerical simulations have been carried out with the adjusted model, first using the monthly time series of rainfall and temperatures at the Barcelonnette climatic station (1971-2000) and secondly, using the monthly time series provided by a climatic model of global change downscaled at the local scale of the Barcelonnette basin (2031-2060). The data used are those of Buma and Dehn (1998). Figure 14 demonstrates the reconstitution of the earthflow's hydrological behaviour. The results must be analysed cautiously, firstly because this approach presupposes that the geometry of the moving mass does not vary over the simulated period, and secondly because of the extreme variability of the outputs of Global Change Models. It seems that over the period from 1971 to 2000 the general trend (two recharge episodes a year, higher groundwater levels in winters with a great amount of snow) is identical with that recorded in the period from 1996 to 2001. It is remarkable to observe that the period from 1975 to 1981 presents a succession of high groundwater levels, which also corresponds to the earthflow's fastest period of runout (Maquaire *et al.*, 2001). In the period from 2031 to 2060 there is a decrease in the average groundwater level of the earthflow. On the long-term, the series also demonstrate a complete change in the earthflow's behaviour with many years showing a single recharge episode. The return frequency of high ground water levels (higher than the movement's acceleration threshold) would thus tend to diminish.

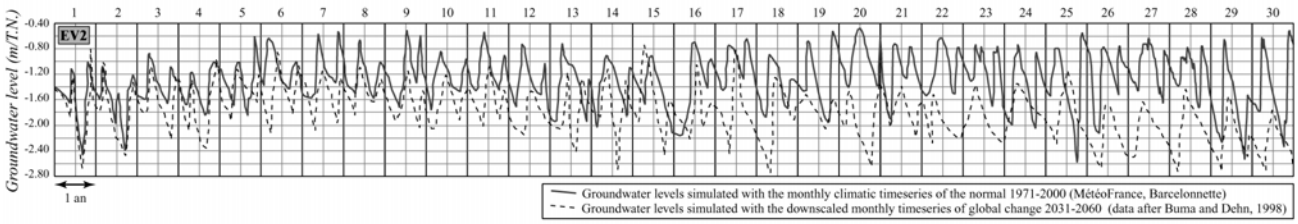

Figure 14. Simulation of the earthflow's hypothetical hydrological regime over the periods from 1971 to 2000 and 2031 to 2060 assuming the climatic change scenario proposed by Dehn and Buma (1998) for the Barcelonnette Basin.

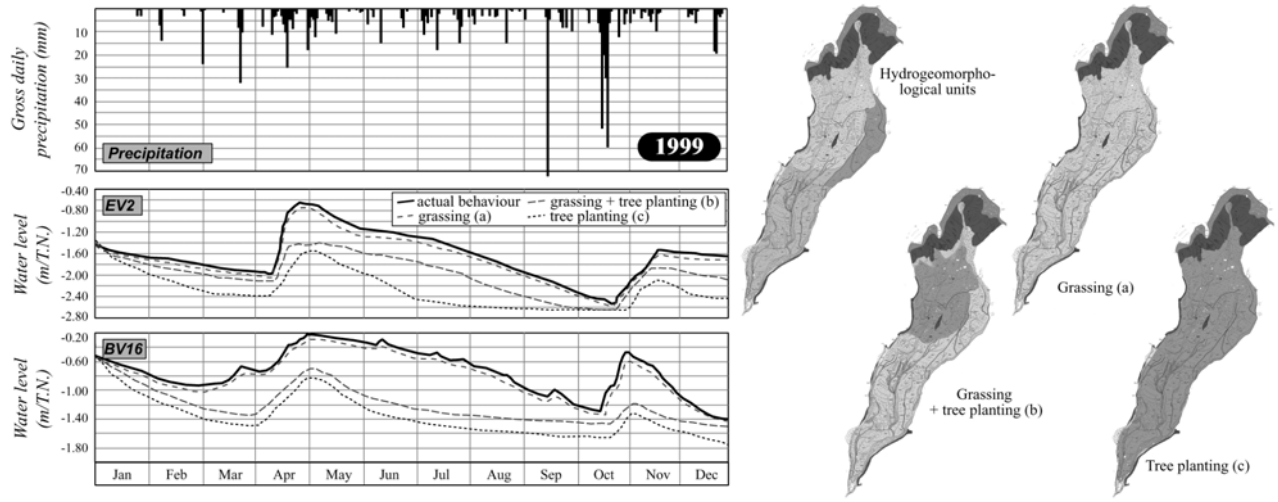

Figure 15. Influence of revegetalisation on the hypothetical hydrological behaviour of the earthflow.

7.2 *Behaviour of the flow under vegetalisation*

A second practical example is the simulation of the earthflow's hypothetical hydrological behaviour in the case of vegetalisation. The effect of artificial revegetalisation through biological engineering can therefore be assessed with a view to reducing the risk.

In order to do so a module representing the manner in which the vegetal cover intercepts rainfall (i.e. a fraction of the gross rainfall function of the foliar index) and an evapotranspiration module (fraction of the potential evapotranspiration reduced by a scale factor k_c, representing the various vegetal covers) has been integrated into the model (Van Beek, 2002).

Three scenarios of revegetalisation have been tested: a complete re-seeding of the earthflow with grass, total reforestation with conifers (20-year-old black pines), and a mixed revegetalisation (reforestation upstream/grass downstream). The simulations were carried out on the year 1999 (Fig. 15). If the influence of re-seeding with grass is almost negligible on the hydrological regime the reforestation considerably lessens the extent of the annual variations and lowers the maximum piezometric level by around 0.80m. The rate of drainage is also changed. The spatial location of populations can also be optimized. It appears that reforestation sole upstream of the earthflow causes a decrease in the water level of around 0.50 m.

8 CONCLUSION

This paper describes a first attempt on the hydrological modelling of clay-shales fast-moving earthflows, taking the Super-Sauze earthflow as representative. The earthflow behaviour is governed by seasonal pore pressure fluctuations inducing long-term movement thanks to the stress changes.

To understand the influence of rainfall recharge on spatially variable ground water flow, we have collected detailed rainfall, and ground-water data. On the basis of our analyses, we infer that persistent downward hydraulic gradients, unsaturated ground-water storage, propagation and attenuation of rainfall-induced pore-pressure waves, and near surface ground water circulation influence the landslide motion profoundly. This complex time-dependent behaviour can be reproduced by a distributed physically-based hydrological model.

The model outputs are quite sensitive to changes in the effective porosity values and conductivity values. Moreover, at this stage of development the recharge by the fissures seems very low, and some specific research should be performed on that topic. Also, considerable simplification is introduced by using constant porosity values instead of transient values as swell-shrink behaviour of the marls or compaction process due to the movement may change the porosities of the layers. The model has proven its capabilities to capture all the necessary physical phenomena with sufficient accuracy to simulate the hydrological behaviour over long periods, to give a quantitative description of triggering events, to locate 'saturated' zones and to provide information for managing such phenomenon. The expert therefore has a new and relatively realistic tool with which to assess the risk.

It should be recalled that this type of model is only one of the tools available to the expert to check his predictions (depending on his intuition, his experience and the field observations). The model does not claim to offer the truth; nevertheless it provides a means of arriving at it and above all it can be used to establish the size of certain parameters by reducing the subjectivity of assessments. Landslide hydrological models seem relatively 'mature' today, but they must be validated and transposed and research must be undertaken on the coupling between hydrology and mechanics for this complex type of landslide.

ACKNOWLEDGMENTS

This program was supported by the European Community in the framework of the NEWTECH Project, and by Centre National de la Recherche Scientifique (CNRS) within the framework of INSU-PNRN (Contract: 97/99-34MT and ECLAT (Ecoulement, initiation et Contribution des LAves Torrentielles dans les bassins marneux)) and the French Ministry of Research within the ACI-CatNat Contract MOTE (MOdélisation, Transformation, Ecoulement des coulées boueuses dans les marnes). Contribution INSU N° 342. Contribution EOST N° 2003.042-UMR7516. The authors wish to thank D. Herrmann, J. Genet, S. Pierre, A. Puissant, A. Remaître, A. Ritzenthaler, M. Schmutz, O. Trisse, E. Truchet, S. Velcin and D. Weber for their precious help in the field, Professor J.-C. Flageollet who encouraged this research, and M. Trautmann for her assistance in the laboratory tests. Very special thanks are due to Mrs. M. Nelson for the reviewing of the English version of the paper.

REFERENCES

Ambroise, B. 1999. *La Dynamique du Cycle de l'Eau dans un Bassin-Versant. Processus, Facteurs, Modèles*. Bucarest: Editions *H*G*.A.

Anderson, M.P., Woessner, W.W., 1991. *Applied Groundwater Modelling. Simulation of Flow and Advective Transport.* London: Academic Press.

Anderson, M.G., Kemp, M.J. 1988. *Application of soil water finite difference model to slope stability problems*. In Bonnard, C. (Ed.), Landslides, Proceedings of the 5th International Symposium on Landslides, 525-531. Rotterdam: Balkema.

Angeli, M.G., Buma., J., Gasparetto, P., Pasuto, A. 1998. A combined

hillslope hydrology/stability model for low gradient clay slopes in the Italian Dolomites. *Engineering Geology,* 49: 1-13.

Antoine, P., Giraud, A., Meunier, M., Van Asch, Th.W.J. 1995. Geological and geotechnical properties of the 'Terres Noires' in the south-eastern France: weathering, erosion, solid transport and instability. *Engineering Geology,* 40: 223-234.

Bogaard, T.A., Antoine, P., Desvarreux, P., Giraud, A., Van Asch, Th.W.J. 2000. The slope movements within the Mondorès graben (Drôme, France): the interaction between geology, hydrology and typology. *Engineering Geology*, 55(4): 297-312.

Bonomi, T., Cavallin, A. 1999. Three-dimensional hydrogeological modelling application to the Alverà mudslide (Cortina d'Ampezzo, Italy). *Geomorphology*, 30(1-2): 189-199.

Brooks, S.M., Crozier, M.J., Preston, N.J., Anderson, M.G. 2002. Regolith stripping and the control of shallow translational hillslope failure: application of a two-dimensional coupled soil hydrology-slope stability model, Hawke's Bay, New Zealand. *Geomorphology*, 45(3-4): 165-179.

Brunsden, D. 1999. Some geomorphological considerations for the future development of landslide models. *Geomorphology*, 30(1-2): 13-24.

Collinson, A.J.C., Anderson, M.G. 1996. Using a combined slope hydrology and stability model to identify suitable conditions for landslide prevention by vegetation cover in the humid tropics. *Earth Surface Processes and Landforms*, 21**:** 737-747.

Caris, J.P.T., Van Asch, Th.W.J. 1991. Geophysical, geotechnical and hydrological investigations of a small landslide in the French Alps. *Engineering Geology*, 31: 249-276.

Corominas, J., 1998. *New technologies for landslide hazard assessment and management in Europe*. Final Report, EC-Programme NEWTECH ENV-CT96-0248. Brussels: European Commission.

Farrel, D., Larson, W. 1972. Modelling the pore structure of porous media. *Water Resources Research*, 3: 699-705.

Flageollet, J.-C., Malet, J.-P., Maquaire, O. 2000. The 3-D structure of the Super-Sauze earthflow: a first stage towards modelling its behaviour. *Physics and Chemistry of the Earth,* 25(9): 785-791.

Freeze, R.A. 1987. *Modeling interrelationships between climate, hydrology and hydrogeology and the development of slopes*. In Anderson, M.G., Richards K.S. (Eds), Slope Stability, 224-265, London: Wiley & Sons.

Freeze, R.A., Cherry, J.A. 1979. *Groundwater*. Englewood Cliffs: Prentice-Hill.

Giusti, G., Iaccarino, G., Pellegrino, A., Picarelli, L., Russo, C., Urciuoli, G. 1996. *Kinematic features of earthflows in Southern Appenines, Italy*. In Sennesset, K. (Ed), Landslides. Proceedings of the 7th International Symposium on Landslides, 457-462. Rotterdam: Balkema.

Haneberg, W.C. 1991. Pore pressure diffusion and the hydrologic response of nearly saturated, thin landslide deposits to rainfall. *Journal of Geology*, 99(8): 886-892.

Hodge, R.A.L., Freeze, R.A. 1977. Groundwater flow systems and slope stability. *Canadian Geotechnical Journal*, 14: 466-476.

Hungr, O., Evans, S.G., Bovis, M.J., Hutchinson, J.N. 2001. A review of the classification of landslides of the flow type. *Environmental and Engineering Geoscience,* 7: 221-238.

Iverson, R.M., Reid, M.E., LaHusen, R.G. 1997. Debris-flow mobilization from landslides. *Annual Revue on Earth and Planetary Science,* 25: 85-138.

Iverson, R.M., Major, J.J. 1986. Groundwater seepage vectors and the potential for hillslope failure and debris flow mobilization. *Water Resources Research*, 22: 1543-1548.

Keefer, D.K., Johnson, A.M. 1983. Earthflows morphology, mobilization and movement. *U.S. Geological Survey Professional Paper 1264.*

Malet, J.-P., Hartig, S., Calais, E., Maquaire, O. 2000. Apport du GPS au suivi en continu des mouvements de terrain. Application au glissement-coulée de Super-Sauze (Alpes-de-Haute-Provence, France), *Comptes-Rendus de l'Académie des Sciences*, 331: 175-182.

Malet, J.-P., Maquaire, O., Calais, E. 2002. The use of Global Positioning System for the continuous monitoring of landslides. Application to the Super-Sauze earthflow (Alpes-de-Haute-Provence, France). *Geomorphology,* 43: 33-54.

Malet, J-P., Maquaire, O., 2003. *Black marl earthflows mobility and long-term seasonal dynamic in southeastern France).* In Picarelli, L. (Ed.), Proceedings of the International Conference on Fast Slope Movements: Prediction and *Prevention for Risk Mitigation*, 333-340. Bologna: Pàtron Editore.

Malet, J.-P., Locat, J., Remaître, A., Maquaire, O. 2003a. *Dynamics of distal debris-flow induced in clayey earthflows. Implications for hazard assessment.* In Picarelli, L. (Ed.), Proceedings of the International Conference on Fast Slope Movements: Prediction and *Prevention for Risk Mitigation*, 341-348. Bologna: Pàtron Editore.

Malet, J.-P., Auzet, A.-V., Maquaire, O., Ambroise, B., Descroix, L., Esteves, M., Vandervaere, J.-P., Truchet, E. 2003b. Soil surface characteristics influence on infiltration in black marls: application to the Super-Sauze earthflow (southern Alps, France). *Earth Surface Processes and Landforms*, 28(5): 547-564.

Malet, J.-P., Locat, J., Remaître, A., Maquaire, O. (in press). Triggering conditions of debris-flows associated to complex earthflows. The case of the Super-Sauze earthflow (South Alps, France). *Geomorphology*, 18p (in press).

Maquaire, O., Flageollet, J.-C., Malet, J.-P., Schmutz, M., Weber, D., Klotz, S., Albouy, Y., Descloîtres, M., Dietrich, M., Guérin, R., Schott., J.-J. 2001. Une approche multidisciplinaire pour la connaissance d'un glissement-coulée dans les marnes noires (Super-Sauze, Alpes-de-Haute-Provence, France). *Revue Française de Géotechnique,* 95/96: 15-31.

Maquaire, O., Malet, J.-P., Remaître, A., Locat, J., Klotz, S., Guillon, J. Instability conditions of marly hillslopes, towards landsliding or gullying? The case of the Barcelonnette basin, South East France. *Engineering Geology,* 22p (in press).

Marquardt, D.W. 1963. An algorithm for least-squares estimation of non-linear parameters. *Journal of the Society for Industrial and Applied Mathematics.* 11: 431-441.

Martinec, J., Rango, A. 1986. Parameter values for snowmelt-runoff modelling. *Journal of Hydrology*, 84: 197-219.

Merrien-Soukatchoff, V. 2002. *Éléments de réflexion sur la qualité des modélisations en hydrogéotechnique*. Mémoire d'Habilitation à Diriger des Recherches, Nancy : Institut National Polytechnique de Lorraine.

Miller, D.J., J. Sias. 1998. Deciphering large landslides: linking hydrological groundwater and stability models through GIS. *Hydrological Processes*, 12: 923-941.

Millington, R.J., Quirk, J.P. 1961. Permeability of porous solids. *Transactions of the Faraday Society*, 57: 1200-1207.

Mulder, H.F.H.M., Van Asch, T.W.J., 1988a. A stochastical approach to landslide determination in a forested area. In Bonnard, C. (Ed.), Landslides, Proceedings of the 5th International Symposium on Landslides, 1207-1210. Rotterdam: Balkema.

Mulder, H.F.H.M., Van Asch, Th.W.J., 1988b. On the nature and magnitude of variance of important geotechnical parameters. In Bonnard, C. (Ed.), Landslides, Proceedings of the 5th International Symposium on Landslides, 229-243. Rotterdam: Balkema.

Ng, C.W.W., Shi, Q. 1998. A numerical investigation of the stability of unsaturated soil slopes subjected to transient seepage. *Computers and Geotechnics*, 22(1): 1-28.

Picarelli, L., Mandolini, A., Russo, C. 1999. *Long-term movements of an earthflow in tectonised clay shales*. In Yagi, N., Yamagani, T., Jiang, J.C. (Eds), Slope Stability Engineering, Geotechnical and Geoenvironmental Aspects, 1151-1158. Rotterdam: Balkema.

Ridolfi, L., D'Odorico, P., Porporato, A., Rodriguez-Iturbe, I. 2003. Stochastic soil moisture dynamics along a hillslope. *Journal of Hydrology*, 272(1-4): 264-275.

Salt, G. 1988. *Landslide mobility and remedial measures*. In Bonnard, C. (Ed), Landslides. Proceedings of the 5th International Symposium on Landslides, 757-770. Rotterdam: Balkema.

Schmutz, M., Guerin, R., Maquaire, O., Descloitres, M., Schott, J.-J., Albouy, Y. 1999. Apport de l'association des méthodes TDEM (Time-Domain Electromagnetism) et électrique pour la connaissance de la structure interne du glissement-coulée de Super-Sauze (Bassin de Barcelonnette, Alpes-de-Haute Provence, France). *Comptes-Rendus de l'Académie des Sciences,* 328: 797-800.

Schmutz M. 2000. *Apport des méthodes géophysiques à la connaissance des glissements-coulées développés dans les marnes noires. Application à Super-Sauze (Alpes-de-Haute-Provence, France).* PhD Thesis, Strasbourg: Université Louis Pasteur.

Schmutz, M., Albouy, Y., Guérin, R., Maquaire, O., Vassal, J., Descloîtres, M., Schott, J-J. 2000. Contribution of electrical and TDEM methods employed separately and combined to Super Sauze flow-slide knowledge. *Surveys in Geophysics*, 21: 371-390.

Singh, P., Spitzbart, G., Hübl, H., Weinmeister, H.W. 1997. Hydrological response of snowpack under rain-on-snow events: a field study. *Journal of Hydrology*, 202(1-4): 1-20

Theis, C.V. 1941. The effect of a well on the flow of a nearby stream. *American Geophysical Union Transactions,* 22(3): 734–738

Van Asch, Th.W.J., 1997. *The study of hydrological systems to understand changes in the temporal occurrence of landslides related to climatic changes.* In Dikau, R. (Ed.), The Temporal Stability and Ac-

tivity of Landslides in Europe with Respect to Climatic Change (TESLEC), EC-Programme TESLEC EV5V-CT94-0454, 69-86, Brussels: European Commission.

Van Asch, Th.W.J., Buma, J. 1997. Modelling groundwater fluctuations and the frequency of movement of a landslide in the Terres Noires region of Barcelonnette, France. *Earth Surface Processes and Landforms*, 22:131-141.

Van Asch, Th.W.J., Buma, J., Van Beek, L.H. 1999. A view on some hydrological triggering systems in landslides. *Geomorphology,* 30: 25-32.

Van Beek, L.H., 2002. *The impact of land use and climatic change on slope stability in the Alcoy region, Spain*. Utrecht: Netherlands Geographical Studies.

Van Beek, L.H., Van Asch, Th.W.J. 1999. *A combined conceptual model for the effects of fissure-induced infiltration on slope stability*. In Hergarten, S., Neugebauer, H.J. (Eds), Process Modelling and Landform Evolution, 147-167. Berlin: Springer.

Velcin, S. 1997. Approche hydrogéologique du mouvement de terrain de Super-Sauze (mai 1996 à avril 1997). Master Thesis. Strasbourg: Université Louis Pasteur.

Van Genuchten, M.T. 1980. A closed-form equation for predicting the hydraulic conductivity of unsaturated soils. *Soil Science Society of America Journal,* 44: 892-898.

Weber, D., Herrmann, A. 2000. Reconstitution de l'évolution géomorphologique de versants instables par photogrammétrie numérique: l'exemple du glissement de terrain de Super-Sauze (Alpes-de-Haute-Provence, France). *Bulletin de la Société Géologique de France*, 171(6): 637-648.

Wesseling, C.G., Karssenberg, D., Van Deursen, W.P.A., Burrough, P.A. 1996. Integrating dynamic environmental models in GIS: the development of a dynamic modelling language. *Transactions in GIS*, 1: 40-48.